

Thermal conductivity of high purity synthetic single crystal diamonds

A. V. Inyushkin* and A. N. Taldenkov

National Research Center Kurchatov Institute, Moscow 123182, Russia

V. G. Ralchenko† and A. P. Bolshakov

*A. M. Prokhorov Institute of General Physics RAS, Moscow 119991, Russia
and Harbin Institute of Technology, Harbin 150080, People's Republic of China*

A. V. Koliadin and A. N. Katrusha

New Diamond Technology LLC, St. Petersburg, Sestroretsk 197706, Russia

(Received 14 November 2017; revised manuscript received 30 March 2018; published 23 April 2018)

Thermal conductivity of three high purity synthetic single crystalline diamonds has been measured with high accuracy at temperatures from 6 to 410 K. The crystals grown by chemical vapor deposition and by high-pressure high-temperature technique demonstrate almost identical temperature dependencies $\kappa(T)$ and high values of thermal conductivity, up to $24 \text{ W cm}^{-1} \text{ K}^{-1}$ at room temperature. At conductivity maximum near 63 K, the magnitude of thermal conductivity reaches $285 \text{ W cm}^{-1} \text{ K}^{-1}$, the highest value ever measured for diamonds with the natural carbon isotope composition. Experimental data were fitted with the classical Callaway model for the lattice thermal conductivity. A set of expressions for the anharmonic phonon scattering processes (normal and umklapp) has been proposed which gives an excellent fit to the experimental $\kappa(T)$ data over almost the whole temperature range explored. The model provides the strong isotope effect, nearly 45%, and the high thermal conductivity ($>24 \text{ W cm}^{-1} \text{ K}^{-1}$) for the defect-free diamond with the natural isotopic abundance at room temperature.

DOI: [10.1103/PhysRevB.97.144305](https://doi.org/10.1103/PhysRevB.97.144305)**I. INTRODUCTION**

Diamond in the form of a bulk crystal has a very high thermal conductivity $\kappa(T)$ at room temperature, however, its value depends strongly on impurity content and crystal lattice imperfections. For example, nitrogen, which can present in a large concentration in diamonds [1], up to 0.25 at.%, reduces the thermal conductivity by several times [2–9]. Also, diamond shows a strong isotope effect in thermal conductivity: eliminating of isotopic mass disorder in the crystal lattice with the natural carbon isotopes abundance (98.93% ^{12}C and 1.07% ^{13}C) by using the isotopically enriched carbon-12 for the diamond synthesis increases the value of thermal conductivity up to 50% at room temperature [10–13,15]. The highest observed value of thermal conductivity for natural high-quality type IIa diamond, $25 \text{ W cm}^{-1} \text{ K}^{-1}$, was reported by Berman and Martinez [16] in 1976, and has not been confirmed until now. In most publications on thermal conductivity of pure single crystalline diamonds [2–4,7–10,12,13,15], the values of κ are 10%–20% below the Berman and Martinez value. This discrepancy means that a significant uncertainty exists in the magnitude and temperature dependence of thermal conductivity for highly pure and low-defect single crystal of diamond that results in a corresponding inaccuracy in assessment of intrinsic phonon scattering processes in diamond.

The key reasons for the high diamond thermal conductivity are well known: the small carbon atomic mass, the strong interatomic bonding in a simple diamond crystal lattice, and low anharmonicity of the interatomic potential [3]. Several theoretical approaches have been used in an attempt to describe the temperature dependence of the thermal conductivity $\kappa(T)$ of single crystalline diamond. Among them are different modifications of the Callaway theory [17] (see the brief review by Berman [18], and Refs. [19,20]), *ab initio* numerical solutions of the Boltzmann transport equation [21–25], and the kinetic-collective model [26]. The high sensitivity of thermal conductivity of diamond to the lattice defects originates from the unusually weak umklapp three-phonon scattering processes near the room temperature [22]. Besides, the interaction of acoustic heat-carrying phonons with optical phonons plays a very important role in thermal conductivity at room and higher temperatures. Recent calculations [27] using *ab initio* Green's function approach show that nitrogen impurities and vacancies are very effective phonon scatterers in diamond, whereas estimations based on the Born approximation underestimate the rate of phonon scattering by nitrogen impurities and vacancies by factors of 3 and 10, respectively.

To test modern theories of heat conduction in crystals, which provide with numerical data for thermal conductivity, a comparison of theoretical results with accurate experimental data in the most simple case of chemically pure and structurally perfect crystals is one of the best ways. In the last decade, the diamond growth techniques demonstrated a remarkable progress [28] resulting in synthesis of chemically very pure bulk single crystals with nitrogen content below 1 ppb (Ref. [29]) and

*inyushkin_av@nrcki.ru

†vg_ralchenko@mail.ru

superior crystal lattice perfection [30]. However, the accurate measurements of $\kappa(T)$ for high-quality diamond from very low to high temperatures are still rare. In this work, we revisit experimental study of thermal conductivity in highly pure state-of-the-art synthetic single crystalline diamonds and present precise experimental data in a wide temperature range from 6 to 410 K. Three different crystals, all of type IIa, were investigated: two chemical vapor deposition (CVD) and one high-pressure high-temperature (HPHT) crystal. The data obtained are analyzed within the single-mode phonon relaxation time approximation using the phenomenological Callaway theory of low-temperature thermal conductivity [17] in its simple original form. We have achieved a very well fit of the theoretical model to experimental data over the entire temperature range using refined parameters for the phonon-phonon scattering processes. This model predicts very high magnitude of thermal conductivity $\kappa(T)$, about $700 \text{ W cm}^{-1} \text{ K}^{-1}$ in maximum at $T \approx 70 \text{ K}$, for the perfect defect-free diamond enriched with ^{12}C to 99.9%.

II. EXPERIMENT

All single crystalline diamonds studied in this work were synthetic ones with natural isotopic composition of carbon. One specimen (denoted NE6) in the form of a rectangular parallelepiped with dimensions $4.20 \times 4.10 \times 0.50 \text{ mm}^3$ was the commercial electronic-grade CVD crystal from Element Six LLC with the concentration of substitutional neutral nitrogen $[\text{N}_s] < 5 \text{ ppb}$ and boron $[\text{B}] < 1 \text{ ppb}$ according to producer information [29]. Two large faces were $\{100\}$ oriented: the long edges had orientation along $[110]$ axis. The single crystal HPHT diamond was produced by New Diamond Technology Company Ltd. (St. Petersburg, Russia) [31]. The sample NDT from this crystal in the form of rectangular plate had dimensions $4.51 \times 4.50 \times 0.54 \text{ mm}^3$ with polished large $\{100\}$ faces, and the same orientation as NE6. It contained nitrogen and boron in concentrations below 5 ppb each, as was evaluated from optical absorption spectra in UV and IR ranges. The third crystal was grown homoepitaxially on a HPHT substrate at General Physics Institute RAS (Moscow, Russia) using a microwave plasma-assisted CVD process [32]. The bar-shaped specimen GPI had the length 7.25 mm with orientation along $[110]$ crystal axis, average thickness 0.32 mm, and two large $\{100\}$ faces with the width 1.54 mm. The concentrations of nitrogen and boron were estimated from optical absorption spectra (according to procedure described in Refs. [33,34]) to be less than 110 and 5 ppb, respectively. The large $\{100\}$ faces were polished to the roughness of $\text{Ra} < 5 \text{ nm}$ (NDT and NE6 samples) and $\text{Ra} < 7 \text{ nm}$ (GPI). The small faces were laser cut surfaces for all three samples; they were not polished.

The thermal conductivity was measured by a steady-state longitudinal heat flow method. A constant heat current was directed along the long axis of a sample, the resulting temperature gradient was measured with a thermopile consisting of 10 type E (chromel/constantan) thermocouples. The chromel and constantan wires (from OMEGA Engineering, Inc.) had a diameter of $25 \mu\text{m}$. The thermocouple has been calibrated by us with using a couple of calibrated Cernox thermometers (LakeShore CX-1050-SD). The thermopower $S(T)$ of this

thermocouple relative to the standard dependence for the type E thermocouple amounts to about 0.95 at $T > 273 \text{ K}$, 0.96 in the range from 35 to 273 K, and 0.9 at $4 \text{ K} < T < 12 \text{ K}$. The thermopile was attached to the large face of the sample with a U-shaped spring clip. The distance (along the sample surface) between the thermopile legs was about 2.5 mm with uncertainty of $\pm 50 \mu\text{m}$, which represented the major source of systematic experimental error ($\pm 2\%$) in thermal conductivity.

The heat was generated in the chip-resistor mounted to one end of the sample with a GE7031 varnish. The opposite end of the sample was contacted to a heat sink, a copper block with regulated temperature. The mechanical connection was achieved by pressing the sample to the copper block with a force applied by a flat bronze spring to the sample end that carried the heater. To improve the contact thermal conductance, a thin indium metal foil was placed in-between the sample end and the heat sink. The sample GPI in the form of long bar was attached to the heat sink with a crocodile clip. To measure the temperature gradient in the sample, the two-step procedure similar to that proposed by Cappelletti and Ishikawa [35] was used. At the first step with the sample heater off and at the second with the heater on, the temperature of the heat sink was controlled to be the same within $\sim 10^{-5} \text{ T}$. The temperature gradient was determined from the difference between thermopile voltages measured at the heater on and off. The temperature drop over the contact sample/sink was measured with a separate type E thermocouple. In the case of the heater on, the contact temperature drop increased from about 0.1 K at lowest temperatures to about 0.3 K at 50 K and kept almost constant above. The temperature difference between the thermopile legs upon the heat flow through the sample ranged from a few millikelvin (for temperatures from 6 K to conductivity maximum temperatures) to several tens millikelvin (at $T > 150 \text{ K}$). The magnitude of this temperature difference was restricted from above by the relatively high thermal resistance between the heat sink and the liquid helium bath at low temperatures. So small temperature gradient makes the measurements for millimeter-scale sample very difficult; this could explain why the accurate experimental data for $\kappa(T)$ are still scarce. We used the Keithley 2002 multimeter with Keithley 1801 preamplifier to measure the thermopile voltage within 1 nV (standard deviation), which corresponds to the temperature noise of approximately 0.05 mK at 5 K, 0.01 mK at 30 K, and 0.003 mK above 100 K. However, the fluctuating and drifting spurious voltage in the thermopile extension wires and the finite-temperature fluctuations of the heat sink increased the temperature noise very much. The temperature difference was determined as an average over the 200 readings, so the random error was reduced by about one order of magnitude. The drifting spurious voltage was the main source which determined the random error of conductivity measurements. To reduce this error at $T \leq 10 \text{ K}$, the conductivity measurements were performed up to 10 times at a given temperature. The following random errors in the thermal conductivity measurements were achieved: 10% at 6 K, 2% at 10 K, then the error decreased to 1% at 100 and 0.1% at $T > 300 \text{ K}$.

To minimize the systematic errors of measurements, the following measures were realized. The measurements were carried out in vacuum (the pressure was typically $< 5 \times 10^{-6} \text{ mbar}$) to exclude the conduction through the residual

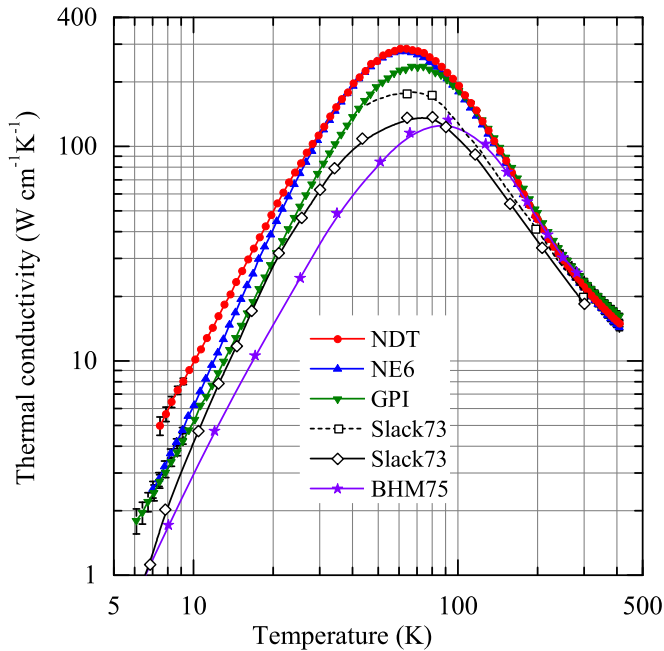


FIG. 1. Thermal conductivity of type IIa single crystalline diamonds versus temperature. This work: circles and triangles. Slack73: experimental data [3] for two HPHT diamonds with cross sections $3.4 \times 3.4 \text{ mm}^2$ (open squares) and $1.0 \times 1.0 \text{ mm}^2$ (open diamonds), and with $[N] = 0.1$ and 50 ppm, respectively. BHM75 (stars): measured data [4] for natural diamond with cross section about $1 \times 1 \text{ mm}^2$ and length $\approx 6 \text{ mm}$. The error bars are larger than the symbols size only at temperatures below 9 K.

gas. The sample was placed inside a multilayer radiation shield to minimize radiation losses at $T > 90 \text{ K}$. All electrical leads and the sample clamp were made from low thermal conductive materials with small cross section to minimize the conduction through them. We estimate that the heat lost due to the residual gas and electrical leads was negligible, $< 0.1\%$. The heat lost through the sample clamp (used in measurements of samples NE6 and NDT) was about 1% at 6 K and decreased to below 0.4% at $T > 10 \text{ K}$. The error due to radiation losses could be about 0.5% at 410 K and varied nearly as T^3 with temperature. The systematic errors in calibration of our chromel/constantan thermocouple amounted to 2% at 5 K, reduced to 0.3% at 10 K, and then to 0.1% at $T > 100 \text{ K}$. The total experimental error in determination of absolute value of thermal conductivity is estimated to be 2%–3%, except the lowest and highest temperatures where it is noticeably higher due to a reduced sensitivity of the thermocouple at liquid helium temperatures and a dramatic rise of radiation heat loss from the sample with temperature at $T > 300 \text{ K}$.

III. RESULTS AND DISCUSSION

A. Experimental data

The experimental data for the samples studied in this work at temperatures from 6 to 410 K are presented in log-log scale in Fig. 1. The data for type IIa high-quality single crystalline diamonds from other works [3,4] are also shown here for comparison purposes. The observed dependencies

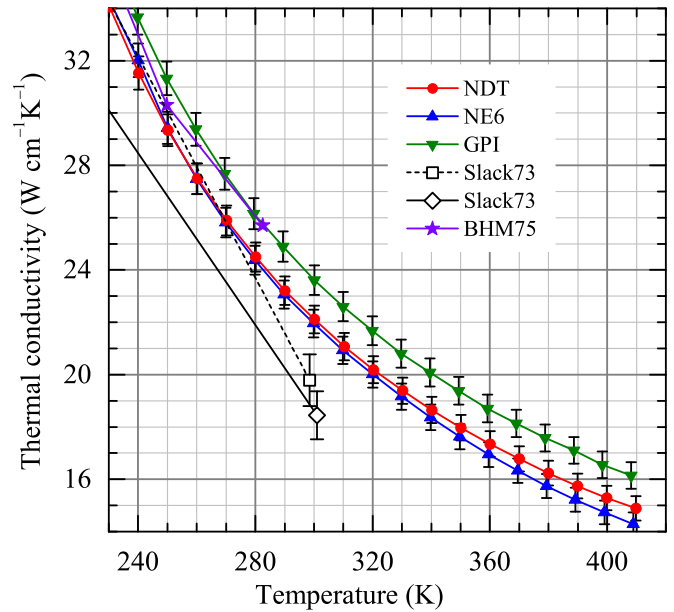


FIG. 2. The temperature dependence of thermal conductivity of diamonds at high temperatures. Symbol designation is as in Fig. 1.

$\kappa(T)$ are characteristic for the phonon thermal conductivity of dielectric crystals. At high temperatures, it is dominated by the anharmonic phonon-phonon scattering processes. These processes weaken with temperature decrease, giving rise to the phonon mean-free path. The phonon free path becomes comparable with sample dimensions at low enough temperature, where $\kappa(T)$ reaches a maximum. The conductivity value near the maximum depends strongly on the impurity content and the concentration of crystal structure defects. At temperatures below the maximum, the behavior of $\kappa(T)$ is determined by the phonon interaction with sample surfaces and subsurface damage layer if the latter exists. For example, if phonons scatter diffusively off the surfaces, the phonon free path is temperature independent and equals approximately to the sample cross-section dimension [36]. In this case, the $\kappa(T)$ varies with temperature as the phonon heat capacity does, i.e., as T^3 .

To highlight the dependencies $\kappa(T)$ at high temperatures, above 230 K, the data are reproduced in a linear scale in Fig. 2. It is seen at high temperatures our data are in a good agreement with the data of Berman *et al.* [4]. At moderate and low temperatures, our data are systematically higher than the literature data [3,4]. These observations unambiguously point to the lower concentration of structural defects and impurities in the samples studied in this work.

The measured $\kappa(T)$ curves for HPHT and CVD samples (NDT and NE6) of similar orientation, surface treatment, and close dimensions practically coincide, within experimental errors, in the whole measurement temperature range, except the low temperatures ($< 30 \text{ K}$). At conductivity maximum at 63 K, where crystal lattice defects strongly influence the magnitude of thermal conductivity, the almost identical values κ_{max} of 285 and 278 $\text{W cm}^{-1} \text{K}^{-1}$ are found for these two samples, respectively (see Table I). Since the concentration of chemical impurities and structural defects may be very

TABLE I. The measured values of thermal conductivity at room temperature $RT = 298.15$ K and in maximum with corresponding values of T_{\max} .

Sample	κ (RT) (W cm ⁻¹ K ⁻¹)	κ_{\max} (W cm ⁻¹ K ⁻¹)	T_{\max} (K)
GPI (CVD)	23.8 ± 0.5	235 ± 7	70.0
NDT (HPHT)	22.3 ± 0.5	285 ± 7	63.6
NE6 (CVD)	22.1 ± 0.5	278 ± 7	62.1
Slack73 ^a (HPHT)	20.0 ± 1 ^b	175 ± 9	65

^aData from Ref. [3].

^bThe value for $T = 300$ K.

different, but are low, and the samples have similar form and sizes, this identity in κ_{\max} indicates that the rates of point-defect scattering are nearly the same in these samples. The common for both samples scattering from impurity isotope ¹³C is, evidently, much stronger than scattering processes from any other point defects, and determines the value of κ_{\max} . It is worth noting that the measured κ_{\max} values are the record high for diamonds with the natural isotopic composition, demonstrating a more than 60% gain with respect to the data reported by Slack [3].

The $\kappa(T)$ for sample NE6 varies steeper than for NDT at temperatures below 20 K. The temperature exponent n , in dependence $\kappa(T) \sim T^n$, is about 2.75 for NE6 in the interval 10–20 K. These values are very close to 3, the value expected for the exponent in the boundary scattering regime with the scattering rate independent of phonon frequency, this being characteristic to $\kappa(T)$ for temperatures below T_{\max} . For sample NDT, the mean value of n is lower, 2.33 at temperatures from 10 to 20 K. We ascribe tentatively the different behavior of $\kappa(T)$ for these two samples at low temperatures to a difference in the phonon boundary scattering due to specific polishing procedures of the diamond producers. Indeed, not only the surface roughness, but also the properties of the subsurface damaged layer induced by the polishing, the thickness of which can be of the order of 1 μm [37], may play a role in the phonon scattering. It seems that the contribution of the specular scattering of phonons at the sample surface is much more significant in the case of specimen NDT. For the sample GPI, the exponent n is 2.50 in this temperature range, in-between values for the samples NDT and NE6.

The sample GPI has the $\kappa(\text{RT}) = 23.8$ W cm⁻¹ K⁻¹, about 7% exceeding those for our other two samples. This value is one of the highest for thermal conductivity of synthetic diamonds at room temperature. Note that for single crystalline CVD diamonds, the thermal conductivity as high as 23.0 ± 3.3 W cm⁻¹ K⁻¹ at RT (Ref. [32]) and even 25 ± 2.5 W cm⁻¹ K⁻¹ (Ref. [38]) have been reported, but in both those works a laser-flash technique was used for the measurements, with accuracy five to six times worse compared to our steady-state method. Since the sample GPI exhibited the enhanced nitrogen content compared to other two samples, its superior conductivity looks surprising. It has a smaller cross section. For smaller cross-sectional dimensions, the boundary scattering rate is higher, and, consequently, the thermal conductivity is lower in the boundary scattering regime [36].

TABLE II. Dimensions of the samples and their Casimir lengths. L_{th} is a sample thermal length (the length over which the temperature gradient is nonzero), c_1 is the correction factor due to deviation of the sample cross section from the square shape, c_2 is the correction factor due to finite length of the sample, $l_C^0 = 1.115 (d_1 \times d_2)^{1/2}$, l_C is the corrected Casimir length.

Sample	d_1 (mm)	d_2 (mm)	L (mm)	L_{th} (mm)	$l_C^{(0)}$ (mm)	c_1	c_2	l_C (mm)
GPI	0.32	1.54	7.25	6.2	0.79	0.871	0.906	0.62
NDT	0.54	4.50	4.51	4.51	1.74	0.781	0.778	1.06
NE6	0.50	4.10	4.20	4.20	1.60	0.784	0.780	0.98

It is for this reason the $\kappa(T)$ for GPI is systematically lower than for our other two samples below conductivity maximum. However, at room temperature for samples of millimeter size the boundary scattering does not contribute sizably to the thermal conductivity. The higher $\kappa(\text{RT})$ for sample GPI may originate from the lower concentration of lattice defects in it, such as vacancies, stacking faults, dislocations, etc., in spite of rather high impurity abundance. Therefore, we suggest that ultimate value of $\kappa(\text{RT})$ for perfect diamond with natural isotope composition should exceed 24 W cm⁻¹ K⁻¹.

B. Modeling

At low temperatures, where the phonon scattering due to anharmonic phonon-phonon interactions and phonon interactions with lattice defects and impurities is negligible comparing to the scattering from sample boundaries, the phonon free path becomes of the order of sample dimensions. Casimir [36] has found that in a case of elastically isotropic, infinitely long rod, having a square cross section, and diffusive phonon scattering from the sample surface, the thermal conductivity is given by

$$\kappa(T) = \frac{1}{3} C v_C l_C, \quad (1)$$

where C is the volume specific heat; v_C is the Casimir velocity, which is an average phonon velocity ($v_C = \langle s^{-2} \rangle / \langle s^{-3} \rangle$), $\langle s^{-k} \rangle = 1/3 \sum_i s_i^{-k}$, $k = 2, 3$, s_i is the directional average phase velocity for polarization i ; and l_C is the phonon mean-free path equal to Casimir length. For the rod with square cross section $l_C = 1.115 d$, d is the side dimension. For the rectangular rod with length L and cross section $d_1 \times d_2$, $l_C = c_1 c_2 \times 1.115 (d_1 d_2)^{1/2}$, where $c_1 < 1$ is a correction factor [39] depending on the ratio d_1/d_2 , and the correction factor $c_2 < 1$ for the finite-length rod is $\approx 1 - l_C/L$ in the first approximation [40,41]. The dimensions of the studied samples and parameters of the boundary scattering are listed in Table II. Debye velocity $v_D = 13.36 \times 10^5$ cm/s and Debye temperature $T_D = 2230$ K for diamond were calculated by us from the room-temperature elastic moduli of Vogelgesang *et al.* [42]. The temperature variation of the elastic moduli and density ρ is so small that the changes of v_D and T_D upon cooling to low temperatures are negligible (about 0.1%). Note also that Casimir velocity $v_C = 12.98 \times 10^5$ cm/s, only slightly ($\approx 3\%$) lower than v_D , so we used v_D instead of v_C and other mean phonon

velocities (having omitted the subscript) in our calculations below.

Nepsha *et al.* [43] and Berman [44] have found that normal processes play an important role in thermal conductivity of diamond with natural isotopic composition. Therefore, to analyze experimental data, we used the Callaway expression for thermal conductivity in its original full form [17], which takes into consideration the specific role of normal scattering processes. In this theory, no distinction is made between phonon polarization modes, and the isotropic phonon spectrum with linear dispersion (Debye model) is assumed. The phonon thermal conductivity is a sum of two terms, the Debye (kinetic) term κ_1 and Ziman (drift) term κ_2 :

$$\kappa(T) = \kappa_1 + \kappa_2, \quad (2)$$

where

$$\kappa_1 = G T^3 \langle \tau_C \rangle, \quad (3)$$

$$\kappa_2 = G T^3 \frac{\langle \tau_C / \tau_N \rangle^2}{\langle \tau_C / (\tau_N \tau_R) \rangle}, \quad (4)$$

$$G = \frac{k_B^4}{2\pi^2 \hbar^3 v}. \quad (5)$$

Here, v is a mean phonon velocity, k_B is the Boltzmann constant. The combined relaxation rate τ_C^{-1} is defined by

$$\tau_C^{-1} = \tau_R^{-1} + \tau_N^{-1}, \quad (6)$$

where τ_R^{-1} is the total scattering rate of all resistive processes, and τ_N^{-1} is the rate of the normal processes. The angled brackets $\langle f \rangle$ represent the following operation:

$$\langle f \rangle = \int_0^{T_D/T} \frac{x^4 e^x}{(e^x - 1)^2} f(x) dx, \quad (7)$$

where $x = \hbar\omega/k_B T$, ω is the phonon frequency.

In the fitting of the model to the experimental data, the limited number of phonon scattering processes were taken into consideration: the boundary scattering, the point-defect scattering, and the three-phonon scattering processes. The boundary scattering has the rate $\tau_b^{-1} = v/l_b$. The adjustable parameter l_b is obtained from the fitting procedure: it measures the phonon free path in the boundary scattering regime. The point-defect scattering rate is given by τ_{pd}^{-1} ,

$$\tau_{pd}^{-1} = \tilde{A}_{pd} \omega^4 = A_{pd} x^4 T^4, \quad (8)$$

where A_{pd} is determined by the point-defect properties and their concentration. In the simplest case of isotopic impurity in the long-wavelength approximation [45]

$$\tilde{A}_{pd} = \tilde{A}_{iso} = g_2 \frac{V_0}{4\pi v^3}, \quad (9)$$

$$g_2 = \sum_i f_i (\Delta M_i / M)^2. \quad (10)$$

Here, f_i is the concentration of i th isotope with mass M_i , which differs from the mean mass $M = \sum_i f_i M_i$ by $\Delta M_i = M_i - M$, V_0 is the volume per atom ($5.6736 \times 10^{-24} \text{ cm}^3$ here). For diamond with the natural mixture of carbon isotopes ^{nat}C , $g_2^{(nat)} = 7.39 \times 10^{-5}$, and $A_{iso}^{(nat)} = 4.109 \times 10^{-3} \text{ s}^{-1} \text{ K}^{-4}$.

Evidently, this isotope scattering represents the minimal possible scattering of phonons from point defects, and A_{pd} cannot be less than $A_{iso}^{(nat)}$ in real crystal.

The following expressions were used to calculate the scattering rates for N and U processes:

$$\tau_N^{-1} = \tilde{A}_N \omega^n T^m = A_N x^n T^{n+m}, \quad (11)$$

$$\tau_U^{-1} = \tilde{A}_U \omega^p T^r e^{-T_D/\alpha T} = A_U x^p T^{p+r} e^{-T_D/\alpha T}, \quad (12)$$

where A_N , A_U , and α are adjustable parameters, and n , m , p , r are integers. For real crystal, it is practically impossible to derive exact analytical expressions for three-phonon scattering due to complicated nature of the phonon dispersion relations and a number of contributions from processes involving various polarization combinations (see, for example, Refs. [46–50]). Different expressions for phonon-phonon scattering rates have been used in analysis of experimental data in the frame of the Callaway theory (see, e.g., Refs. [13,19,43,51,52]). Morelli, Heremans, and Slack [19] discussed in detail the anharmonic scattering processes and proposed a simple model for numerical calculations of the phonon-phonon scattering rates. Within the Debye-Callaway model modified to include both transverse (T) and longitudinal (L) phonon modes explicitly, the quantitative account for the observed isotope effect in diamond [12] was obtained using $(n,m|p,r) = (1,4|2,1)$ and $(2,3|2,1)$ for T and L modes, respectively. The combination $(1,3|2,1)$ has been used by Wei *et al.* [13] for isotopically modified single crystal diamond. They have found that a single set of values, $A_N = 1.50 \text{ s}^{-1} \text{ K}^{-4}$, $A_U = 487 \text{ s}^{-1} \text{ K}^{-3}$, and $T_D/\alpha = 670 \text{ K}$, well describes their experimental dependence $\kappa(T)$ and the observed isotope effect at temperatures above 100 K. This combination has been also used by Graebner *et al.* [53] and Inyushkin *et al.* [54] for fitting $\kappa(T)$ measured for polycrystalline diamonds.

The experimental data for diamonds with natural and enriched isotopic compositions from different experiments [11–13] (symbols), and our calculations of $\kappa(T)$ (dotted lines) using the above-mentioned Wei's model for the phonon-phonon scattering rates are displayed in Fig. 3. Also shown here are our experimental data for the CVD sample NE6 (blue triangles) and the theoretical curve calculated with Wei's set of parameters for A_N and A_U , but with adjusted value for l_b , are also shown here (blue dotted line). The calculations have been performed with the parameter of point-defect scattering $A_{pd} = A_{iso}^{(nat)}$, which corresponds to the perfect crystal without chemical impurities and structural defects. These curves denote the upper limit for thermal conductivity of crystals with specified isotope compositions within the frame of this model. It is seen from Fig. 3 that the Wei's set of parameters is inadequate to describe the $\kappa(T)$ for the sample NE6 at temperatures near the conductivity maximum and up to approximately 150 K: the calculated data are much lower than the experimental. It is noteworthy, however, that this set provides a good fit to the $\kappa(T)$ data of different experiments [11–14] in the range $200 < T < 1200 \text{ K}$, a high value for the isotope effect, 35% at room temperature, close to the experimental value (45%–50%), and $\kappa(\text{RT}) \approx 24 \text{ W cm}^{-1} \text{ K}^{-1}$. We think that it is not surprising that the single set of expressions for three-phonon scattering processes can not account for experimental $\kappa(T)$

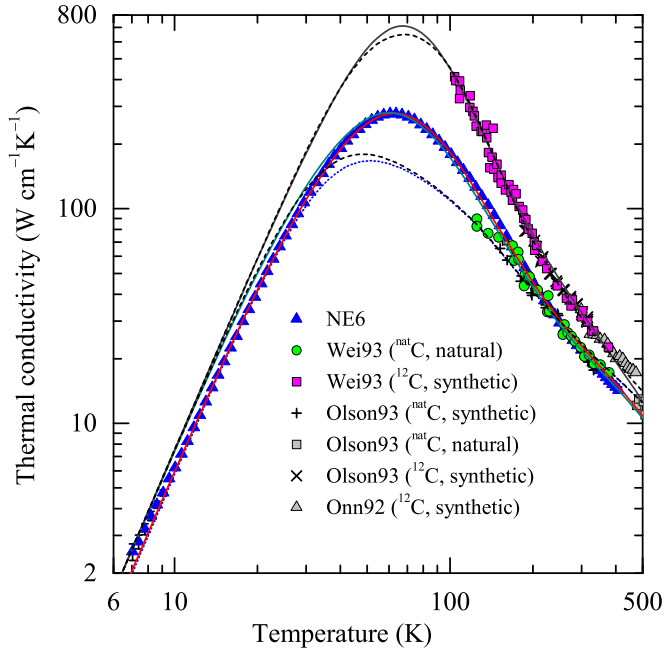


FIG. 3. The temperature dependence of thermal conductivity of single crystalline diamonds: experimental (symbols) and theoretical (lines) data. The dashed lines are calculation results of the Wei's model for their experiment [13] with diamonds with natural ^{nat}C and enriched ^{12}C (99.9%) isotopic compositions; the dotted line is the Wei's model result for our sample NE6; solid lines are the fits to experimental data with our model.

in a very wide temperature interval, from boundary scattering regime to 1200 K for diamond. It is well known (see, e.g., Refs. [49,50,55,56]) that the low- and high-temperature limits for anharmonic scattering rates have different temperature and frequency dependencies.

We have tested several different forms for frequency and temperature dependencies of three-phonon scattering rates in order to obtain the best fit to (i) the experimental data on $\kappa(T)$ for NE6, (ii) the isotope effect (45%–50%), and (iii) the value near $25 \text{ W cm}^{-1} \text{ K}^{-1}$ for highest quality crystal of natural isotopic abundance at room temperature. The following combinations $(n, m|p, r)$ for N - and U -scattering rates have been examined: $(1, 3|2, 1)$, $(2, 2|2, 1)$, $(1, 4|1, 2)$, $(1, 4|1, 3)$, $(1, 4|2, 1)$, $(1, 4|2, 2)$, $(2, 3|2, 1)$, $(2, 3|3, 0)$, $(2, 3|3, 1)$. It has been found that a satisfactory matching can be obtained with the sets $(1, 4|1, 2)$ and $(1, 4|1, 3)$. Both sets give a good fitting to the experimental $\kappa(T)$ and the correct magnitude of isotope effect of about 45% for the defect-free sample at room temperature. The former combination $(1, 4|1, 2)$ seems to be preferable since it provides the higher value of $\kappa(\text{RT})$ as compared to the latter combination. The best fit to the experimental data for sample NE6 using the combination $(1, 4|1, 2)$ is shown by the solid line (red) in Fig. 3. There is a good agreement between the experimental and calculated data over almost entire temperature interval. Only near the interval borders some deviations are seen. At high temperatures, above approximately 400 K, our calculated $\kappa(T)$ is steeper than the experimental one [57]. This can suggest that the anharmonic scattering rates change their temperature dependence significantly with temperature increase to this end

TABLE III. Adjustable parameters of best fittings for samples of single crystal diamond. Parameters $A_N = 3.353 \times 10^{-3} \text{ s}^{-1} \text{ K}^{-5}$, $A_U = 1272 \text{ s}^{-1} \text{ K}^{-3}$, and $T_D/\alpha = 560 \text{ K}$ were obtained with fitting to the data of NE6. The values of isotope scattering parameter A_{iso} were calculated using Eq. (9). η is the root-mean-squared surface roughness.

Sample	A_{pd} ($10^{-3} \text{ s}^{-1} \text{ K}^{-4}$)	A_{iso} ($10^{-3} \text{ s}^{-1} \text{ K}^{-4}$)	l_b (mm)	η (nm)	l_b/l_C
GPI	4.41	4.109	1.54	4.1	2.48
NDT	4.47	4.109	2.57	3.5	2.42
NE6	4.88	4.109	2.62	10.1	2.67
$^{nat}\text{C}^a$	5.80	4.109	3.3 ^b		
$^{12}\text{C}^a$	0.59	0.388	3.3 ^b		

^aSamples from Ref. [13], sample ^{12}C had enrichment of 99.9%.

^bTaken from Ref. [13].

[49,55,56]. A slight downward deviation of the theoretical curve from the experimental $\kappa(T)$ below 10 K can be attributed to the specular scattering of phonons from the sample boundaries; this contribution increases substantially with temperature decrease but it was not accounted for in this version of our model. Adding the dislocation scattering ($\propto \omega$ or ω^3) or the scattering from stacking faults ($\propto \omega^2$) has not improved notably the fit. Note also that the model fit practically does not change with the Debye temperature decrease from 2230 to 1820 K, the cutoff energy of the longitudinal acoustic phonons [57]. The optimal fitting parameters to the data for the sample NE6 are listed in Table III. In fitting the model to the experimental data for other samples, the parameters A_N , A_U , and α were fixed. The model approximates well the experimental $\kappa(T)$; the adjustable parameters for them are also presented in Table III [57]. The sample GPI has the lowest rate of point-defect scattering (in spite of higher nitrogen content) as follows from Table III in accord with its highest conductivity at room temperature. Therefore, the model is compatible with all three samples simultaneously.

We applied our model to the experimental data from Wei *et al.* [13] using our values for A_N and A_U , and the value for l_b from Ref. [13]; A_{pd} was an adjustable parameter. The best fitting results are shown in Fig. 3 by solid lines for the samples with the natural isotope mixture (dark cyan line) and enriched with ^{12}C (black line) composition. It is seen that the quality of this fitting is good, practically the same as that achieved in Ref. [13]. Our results show, however, that the rate of scattering from point defects is substantially higher than that from isotopic defects in these two samples (see Table III). This indicates the relatively high concentration of point defects in the crystals in Ref. [13]: the sample NE6 demonstrates the scattering rate from nonisotope point defects by more than two times lower than for ^{nat}C from Ref. [13], yet comparable with that caused solely by isotopic contribution. Taking into account the high chemical purity of the sample NE6 we have to look for point defects other than nitrogen or boron impurity atoms. We suggest the extra scattering in sample NE6 (aside from the ^{13}C isotope) to originate from vacancies in the crystal lattice. The vacancies are known to be very effective phonon scatterers in crystals [27,58]. According to Ref. [58], the phonon scattering

rate from single vacancies is given by Eq. (8) with

$$\tilde{A}_{\text{pd}} = \tilde{A}_V = \frac{9V_0}{4\pi v^3} c_V, \quad (13)$$

where c_V is the atomic concentration of vacancies. Using A_{pd} from Table III and taking into account the isotope scattering we find that $c_V \approx 1.5$ ppm. Recent accurate theoretical calculations of the phonon scattering from vacancies in diamond [27] show that the scattering rate is about four times higher than that obtained using Eq. (13). Thus, within this theory the concentration of vacancies is estimated to be rather low, 0.4 ppm, the value reasonable for the high-quality diamond crystals (see, e.g., Ref. [59]).

The phonon mean-free path l_b in the boundary scattering regime determined within the fitting to the experimental data for the sample NE6 is 2.6 mm (Table III). This value is substantially larger than the theoretical Casimir free path $l_C = 0.98$ mm calculated from the sample geometry. The same is valid for the samples NDT and GPI. This result is similar to that obtained by Vandersande [6] and Berman [16] for the polished samples of natural diamond, which had not been post-processed after polishing. It was proposed (Ref. [6] and references therein) that the heat-carrying phonons do not reach the sample boundaries, but specular reflected within a thin sub-surface damaged layer. Since the observed $\kappa(T)$ shows nearly T^3 dependence, the rate of this specific scattering is almost independent from the phonon frequency. The mechanism responsible for such phonon specular reflection is still unknown. The phonon focusing (PF) effect can increase substantially, by 10%, the phonon mean-free path comparing with the Casimir length in certain directions in elastically anisotropic crystals below the thermal conductivity maximum [39]. For example, for silicon the calculations of McCurdy, Maris, and Elbaum [39] and recent *ab initio* calculations of Li and Mingo [60] showed approximately 40% enhancement for the [100] direction in comparison with [110] direction in agreement with experimental results [39,61]. The calculations of Kuleyev *et al.* [62] for silicon in the frame of generalized Callaway theory represented very well the experimental data on $\kappa(T)$ below the conductivity maximum. For diamond, the theory [39] predicts about the same value of the PF effect, the conductivity in the [110] direction being close to the Casimir value within few percent in the case of diffuse boundary scattering. The PF effect becomes weaker for finite length samples [63]. The only available experimental data [64] are in qualitative agreement with the theoretical results for diamond. Therefore, taking into account the PF effect in attempt to explain the increased experimental l_b does not reduce the discrepancy between the theoretical and experimental values of free paths in the boundary scattering regime for the samples studied in this work. For all our samples the ratio l_b/l_C falls in the narrow range of 2.4 to 2.7, while Vandersande [6] has found that $2 < l_b/l_C < 3$ for polished natural type IIa diamonds at $T < 20$ K. The good agreement between our model calculations and our precise experimental data over a wide temperature domain suggests that thermal phonons have a single elongate l_b at temperatures above ~ 10 K up to the conductivity maximum at the least.

Adding to our model the possibility for phonons to reflect specular from sample boundaries improves the fitting to

experimental data at lowest temperatures leaving l_b practically unchanged [57]. The scattering rate for this type of boundary scattering is given by [41]

$$\tau_b^{-1} = \frac{v}{l_b} \frac{1-P}{1+P}, \quad (14)$$

where the probability P of specular reflection increases with the decrease of phonon frequency and effective surface roughness η_{eff} (see, e.g., Refs. [65,66]):

$$P = \exp[-(2\eta_{\text{eff}}\omega/v)^2] \quad (15)$$

with $\eta_{\text{eff}} = 2\eta/\pi$, η is the root-mean-squared surface roughness. The parameters of the best fitting for samples studied in this work are presented in Table III. The values for η are rather close (within factor of 2) to the average surface roughness $R_a < 5$ nm specified by the manufactures. Noteworthy, Vandersande [6] has found that the specular reflection of phonons from the polished sample boundaries becomes pronounced in heat transport below about 2 K where the thermal phonon wavelength exceeds 80 nm. This results in the further increase of the phonon mean-free path over the Casimir value with the temperature decrease.

The particular form of the N processes used in this work is characteristic for the Landau-Rumer mechanism [67] of TLL type, the interaction between transverse and longitudinal phonons results in formation of longitudinal phonon. Herring [46] has concluded the same dependence for the N processes for transverse phonons at low temperatures in anisotropic media. Kuleyev *et al.* [68] have suggested that in anisotropic cubic crystals transverse phonons can participate also in the N processes of TTT type, involving only transverse phonons, with the high rate of scattering as compared with the Landau-Rumer case. Since the transverse phonons contribute mostly to the heat flow at low temperatures, one can expect that this form is appropriate in our modeling. The xT^5 form for the N processes has been used by Hass *et al.* [51] in the analysis of isotope effect in thermal conductivity of single crystal diamond using the full version of Callaway theory.

The form for U processes with linear frequency dependence is rather unusual. The ω^2 frequency dependence is commonly assumed (see, for example, Refs. [13,18,19,69]), however, the linear dependence is not excluded theoretically (see Refs. [47,48]). Noteworthy, the usual representation of the anharmonic scattering rate as a product of frequency- and temperature-dependent terms can be considered as an approximation for rather complicated function of phonon frequency and temperature [50]. In this connection, we consider the functional form of τ_U as an empirical one.

The classical Callaway model makes no distinction between transverse and longitudinal phonons. To examine the consequences of this simplification, we have performed additional computations with the model of Morelli, Heremans, and Slack [19], which treats the contributions of longitudinal and transverse phonons explicitly [57]. We have found our simple model to fit the experimental data very well through all the investigated temperature range, not worse than the more complex model.

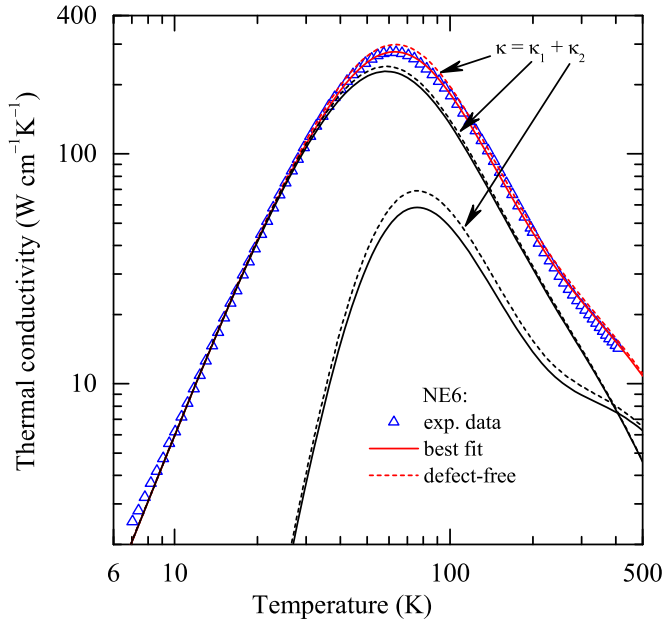


FIG. 4. Contributions of Debye and Ziman terms $\kappa_1(T)$ and $\kappa_2(T)$ to the thermal conductivity of diamond. Triangles are measured data for the sample NE6, solid red and dashed red lines represent the best fit to experimental data and the calculations for defect-free sample, respectively. Two close pairs lines (black) depict $\kappa_1(T)$ and $\kappa_2(T)$, respectively, for the best fit (solid) and for the defect-free (dashed) cases.

Figure 4 shows the calculated temperature dependencies of the Debye $\kappa_1(T)$ and Ziman $\kappa_2(T)$ terms to the total thermal conductivity of the sample NE6. It is seen that $\kappa_1(T)$ dominates over $\kappa_2(T)$ at temperatures $T < 400$ K. However, if point defects are eliminated, it is the increase of $\kappa_2(T)$ that determines mostly the increment in total thermal conductivity at temperatures above the maximum. This result indicates the very important role of normal processes of phonon-phonon scattering in thermal conductivity of diamond with natural isotope abundance [44], which leads to the strong isotope effect in $\kappa(T)$.

It is interesting to note that the calculated dependence $\kappa(T)$ for perfect diamond crystal (dashed red line in Fig. 4) with $A_{pd} = A_{iso}$ (the values for other parameters are taken from Table III) lays only slightly above the best-fit curve (solid red line in Fig. 4) by 8% to 5% at temperatures near and above the maximum: $\kappa_{max} = 299 \text{ W cm}^{-1} \text{ K}^{-1}$ at $T_{max} = 63\text{--}64 \text{ K}$, and $\kappa(\text{RT}) = 24.2 \text{ W cm}^{-1} \text{ K}^{-1}$. Thus, our model indicates that the thermal conductivity of the sample NE6 is close to that of defect-free single crystalline diamond.

Our highest measured $\kappa(\text{RT}) = 23.8 \text{ W cm}^{-1} \text{ K}^{-1}$ is very close, but a bit exceeds by 4% the theoretical upper value of $22.9 \text{ W cm}^{-1} \text{ K}^{-1}$ from the *ab initio* calculations by Broido *et al.* [23] for defect-free diamond with natural isotopic composition. Interestingly, they considered a sample with diameter of 1 mm, very close to the Casimir length for our specimens measured, therefore, the direct comparison of their modeling with the present experiment is justified. In addition, our maximum conductivity $\kappa_{max}(63 \text{ K}) = 285 \text{ W cm}^{-1} \text{ K}^{-1}$ noticeably exceeds also $\kappa_{max} \approx 190 \text{ W cm}^{-1} \text{ K}^{-1}$, obtained

from the first principles by Fugallo *et al.* [24] for diamond with the diameter of 3 mm. This may give grounds to further refine the parameters of the *ab initio* models.

IV. CONCLUSIONS

Accurate data on thermal conductivity $\kappa(T)$ of highly pure single crystals of HPHT and CVD diamond at temperatures from 6 to 410 K have been obtained using newly developed version of the steady-state heat flow method for direct measuring thermal conductivity of extremely high heat conduction materials. The precise data for $\kappa(T)$ with total error less than 3% (random error $\approx 1\%$) were obtained also at temperatures near the conductivity peak, where many previous experiments failed to gather such data. The results, being in general consistency with previously published experimental data for high-quality natural and synthetic diamonds, show one of the highest values for thermal conductivity at room temperature ($23.8 \pm 0.5 \text{ W cm}^{-1} \text{ K}^{-1}$), and the record high conductivity at low temperatures ($285 \pm 7 \text{ W cm}^{-1} \text{ K}^{-1}$ at the peak). Paraphrasing Morelli [70], we have demonstrated that state-of-the-art synthetic diamonds (both CVD and HPHT) are “the final testing ground for determining the intrinsic thermal conductivity of the best heat conductor known to man.”

We have analyzed our measurements of $\kappa(T)$ within the original Callaway theory of thermal conductivity taking into account the boundary scattering, point-defect scattering, and anharmonic three-phonon scattering processes. It was found that the previously widely used expressions for the N and U processes of phonon scattering [13,53,54] cannot describe adequately the obtained experimental extraordinarily high $\kappa(T)$ near the conductivity peak. A set of expressions for anharmonic scattering processes is proposed, that provides a very good agreement of the model with a collection of experimental data for $\kappa(T)$ for $T < 400$ K, presented in this work, as well as reported by other authors, including the data for isotopically enriched diamond. According to the modeling, the values of thermal conductivity of diamonds measured in this work are close to those predicted for a perfect single crystal diamond with natural isotopic composition at temperatures above the conductivity maximum, being only $\approx 5\%$ below the calculated $\kappa(T)$ for ideal crystal (no defects other than ^{13}C isotopes are present) at room temperature. In the boundary scattering regime, the phonon mean-free path exceeds the Casimir length by about 2.4–2.7 times for polished samples; this is a remarkable narrow interval as compared with the results (from 2 to 3 times) reported previously by Vandersande [6] and Berman [16]. At lowest temperatures < 10 K, the specular reflection of phonons at the sample surface becomes sizable on the background of frequency-independent boundary scattering.

ACKNOWLEDGMENTS

This study was partly supported by NRC “Kurchatov Institute,” the Russian Foundation for Basic Research (Grants No. 16-07-00979 and No. 16-07-01188). V.G.R. and A.P.B. acknowledge the support from the Russian Scientific Foundation (Grant No. 14-12-01403-P) of the part of work related to diamond growth and sample preparation.

- [1] W. Kaiser and W. L. Bond, *Phys. Rev.* **115**, 857 (1959).
- [2] R. Berman, E. L. Foster, and J. M. Ziman, *Proc. R. Soc. London A* **237**, 344 (1956).
- [3] G. A. Slack, *J. Phys. Chem. Solids* **34**, 321 (1973).
- [4] R. Berman, P. R. W. Hudson, and M. Martinez, *J. Phys. C: Solid State Phys.* **8**, L430 (1975).
- [5] J. W. Vandersande, *J. Phys. C: Solid State Phys.* **13**, 757 (1980).
- [6] J. W. Vandersande, *Phys. Rev. B* **13**, 4560 (1976).
- [7] E. A. Burgemeister, *Phys. B (Amsterdam)* **93**, 165 (1978).
- [8] E. A. Burgemeister, *J. Phys. C: Solid State Phys.* **13**, L963 (1980).
- [9] D. T. Morelli, T. A. Perry, and J. W. Farmer, *Phys. Rev. B* **47**, 131 (1993).
- [10] T. R. Anthony, W. F. Banholzer, J. F. Fleischer, L. Wei, P. K. Kuo, R. L. Thomas, and R. W. Pryor, *Phys. Rev. B* **42**, 1104 (1990).
- [11] D. G. Onn, A. Witek, Y. Z. Qiu, T. R. Anthony, and W. F. Banholzer, *Phys. Rev. Lett.* **68**, 2806 (1992).
- [12] J. R. Olson, R. O. Pohl, J. W. Vandersande, A. Zoltan, T. R. Anthony, and W. F. Banholzer, *Phys. Rev. B* **47**, 14850 (1993).
- [13] L. Wei, P. K. Kuo, R. L. Thomas, T. R. Anthony, and W. F. Banholzer, *Phys. Rev. Lett.* **70**, 3764 (1993).
- [14] J. W. Vandersande, A. Zoltan, J. R. Olson, R. O. Pohl, T. R. Anthony, and W. P. Banholzer, in *Proceedings of the Seventh International Conference on Phonon Scattering in Condensed Matter, Cornell University, Ithaca, 1992*, edited by M. Meissner and R. O. Pohl (Springer, Berlin, 1993), p. 35.
- [15] A. A. Kaminskii, V. G. Ralchenko, H. Yoneda, A. P. Bol'shakov, and A. V. Inyushkin, *JETP Lett.* **104**, 347 (2016).
- [16] R. Berman and M. Martinez, *Diamond Research 1976*, Suppl. to *Ind. Diam. Rev.* (Industrial Diamond Information Bureau, London, 1976), pp. 7–13.
- [17] J. Callaway, *Phys. Rev.* **113**, 1046 (1959).
- [18] R. Berman, *J. Phys. Chem. Solids* **59**, 1229 (1998).
- [19] D. T. Morelli, J. P. Heremans, and G. A. Slack, *Phys. Rev. B* **66**, 195304 (2002).
- [20] S. Barman and G. P. Srivastava, *J. Appl. Phys.* **101**, 123507 (2007).
- [21] A. Sparavigna, *Phys. Rev. B* **65**, 064305 (2002).
- [22] A. Ward, D. A. Broido, D. A. Stewart, and G. Deinzer, *Phys. Rev. B* **80**, 125203 (2009).
- [23] D. A. Broido, L. Lindsay, and A. Ward, *Phys. Rev. B* **86**, 115203 (2012).
- [24] G. Fugallo, M. Lazzeri, L. Paulatto, and F. Mauri, *Phys. Rev. B* **88**, 045430 (2013).
- [25] J. Ma, W. Li, and X. Luo, *Phys. Rev. B* **90**, 035203 (2014).
- [26] P. Torres, A. Torelló, J. Bafaluy, J. Camacho, X. Cartoixà, and F. X. Alvarez, *Phys. Rev. B* **95**, 165407 (2017).
- [27] N. A. Katcho, J. Carrete, Wu Li, and N. Mingo, *Phys. Rev. B* **90**, 094117 (2014).
- [28] R. S. Balmer, J. R. Brandon, S. L. Clewes, H. K. Dhillon, J. M. Dodson, I. Friel, P. N. Inglis, T. D. Madgwick, M. L. Markham, T. P. Mollart, N. Perkins, G. A. Scarsbrook, D. J. Twitchen, A. J. Whitehead, J. J. Wilman, and S. M. Woollard, *J. Phys.: Condens. Matter* **21**, 364221 (2009).
- [29] Element Six LLC, <http://e6cvd.com/us/material/single-crystalline.html>.
- [30] Y. Shvyd'ko, S. Stoupin, V. Blank, and S. Terentyev, *Nat. Photonics* **5**, 539 (2011).
- [31] U. F. S. D'Haenens-Johansson, A. Katrusha, K. S. Moe, P. Johnson, and W. Wang, *Gems & Gemology* **51**, 260 (2015).
- [32] A. P. Bolshakov, V. G. Ralchenko, V. Y. Yurov, A. F. Popovich, I. A. Antonova, A. A. Khomich, E. E. Ashkinazi, S. G. Ryzhkov, A. V. Vlasov, and A. V. Khomich, *Diam. Relat. Mater.* **62**, 49 (2016).
- [33] S. V. Nistor, M. Stefan, V. Ralchenko, A. Khomich, and D. Schoemaker, *J. Appl. Phys.* **87**, 8741 (2000).
- [34] A. M. Zaitsev, in *Handbook of Industrial Diamonds and Diamond Films*, edited by M. A. Prelas, G. Popovici, and L. K. Bigelow (Marcel Dekker, New York, 1997), Chap. 7, pp. 227–276.
- [35] R. L. Cappelletti and M. Ishikawa, *Rev. Sci. Instrum.* **44**, 301 (1973).
- [36] H. B. G. Casimir, *Physica* **5**, 495 (1938).
- [37] I. Friel, S. L. Clewes, H. K. Dhillon, N. Perkins, D. J. Twitchen, and G. A. Scarsbrook, *Diam. Relat. Mater.* **18**, 808 (2009).
- [38] Y. Yamamoto, T. Imai, K. Tanabe, T. Tsuno, Y. Kumazawa, and N. Fujimori, *Diam. Relat. Mater.* **6**, 1057 (1997).
- [39] A. K. McCurdy, H. J. Maris, and C. Elbaum, *Phys. Rev. B* **2**, 4077 (1970).
- [40] R. Berman, F. E. Simon, and J. M. Ziman, *Proc. R. Soc. London A* **220**, 171 (1953).
- [41] R. Berman, E. L. Foster, and J. M. Ziman, *Proc. R. Soc. London A* **231**, 130 (1955).
- [42] R. Vogelgesang, A. K. Ramdas, S. Rodriguez, M. Grimsditch, and T. R. Anthony, *Phys. Rev. B* **54**, 3989 (1996).
- [43] V. I. Nepsha, V. R. Grinberg, Yu. A. Klyuev, A. M. Naletov, and G. B. Bokii, *Dokl. Akad. Nauk SSSR* **317**, 96 (1991).
- [44] R. Berman, *Phys. Rev. B* **45**, 5726 (1992).
- [45] P. G. Klemens, *Proc. Phys. Soc. London, Sect. A* **68**, 1113 (1955).
- [46] C. Herring, *Phys. Rev.* **95**, 954 (1954).
- [47] P. G. Klemens, in *Solid State Physics*, edited by F. Seitz and D. Turnbull (Academic, New York, 1958), Vol. 7, pp. 1–98.
- [48] M. G. Holland, *Phys. Rev.* **132**, 2461 (1963).
- [49] G. L. Guthrie, *Phys. Rev.* **152**, 801 (1966).
- [50] G. P. Srivastava, in *High Thermal Conductivity Materials*, edited by S. L. Shinde and J. S. Goela (Springer, New York, 2006), pp. 1–35.
- [51] K. C. Hass, M. A. Tamor, T. R. Anthony, and W. F. Banholzer, *Phys. Rev. B* **45**, 7171 (1992).
- [52] M. Asen-Palmer, K. Bartkowski, E. Gmelin, M. Cardona, A. P. Zhernov, A. V. Inyushkin, A. N. Taldenkov, V. I. Ozhogin, K. M. Itoh, and E. E. Haller, *Phys. Rev. B* **56**, 9431 (1997).
- [53] J. E. Graebner, M. E. Reiss, L. Seibles, T. M. Hartnett, R. P. Miller, and C. J. Robinson, *Phys. Rev. B* **50**, 3702 (1994).
- [54] A. V. Inyushkin, A. N. Taldenkov, V. G. Ral'chenko, V. I. Konov, A. V. Khomich, and R. A. Khmel'nitski, *JETP* **107**, 462 (2008).
- [55] R. Berman and J. F. C. Brock, *Proc. R. Soc. London A* **289**, 46 (1965).
- [56] P. C. Sharma, K. S. Dubey, and G. S. Verma, *Phys. Rev. B* **4**, 1306 (1971).
- [57] See Supplemental Material at <http://link.aps.org/supplemental/10.1103/PhysRevB.97.144305> for details of the modeling and additional results.
- [58] C. A. Ratsifaritana and P. G. Klemens, *Int. J. Thermophys.* **8**, 737 (1987).

- [59] W. Zhu, in *Diamond Electronic Properties and Applications*, edited by L. S. Pan and D. R. Kania (Springer, New York, 1995), pp. 175–239.
- [60] W. Li and N. Mingo, *J. Appl. Phys.* **114**, 054307 (2013).
- [61] A. V. Inyushkin, A. N. Taldenkov, J. W. Ager, E. E. Haller, H. Riemann, N. V. Abrosimov, H.-J. Pohl, and P. Becker, *J. Appl. Phys.* **123**, 095112 (2018).
- [62] I. I. Kuleyev, I. G. Kuleyev, S. M. Bakharev, and A. V. Inyushkin, *Phys. Status Solidi B* **251**, 991 (2014).
- [63] A. K. McCurdy, *Phys. Rev. B* **26**, 6971 (1982).
- [64] J. W. Vandersande, *J. Phys. (Paris) Colloq.* **39**, C6-1017 (1978).
- [65] J. M. Ziman, *Electrons and Phonons: The Theory of Transport Phenomena in Solids* (Oxford University Press, Oxford, 2001).
- [66] S. B. Soffer, *J. Appl. Phys.* **38**, 1710 (1967).
- [67] L. Landau and G. Rumer, *Phys. Z. Sowjetunion* **11**, 18 (1937).
- [68] I. G. Kuleyev, I. I. Kuleyev, and I. Y. Arapova, *J. Phys.: Condens. Matter* **20**, 465201 (2008).
- [69] V. I. Nepsha, in *Handbook of Industrial Diamonds and Diamond Films*, edited by M. A. Prelas, G. Popovici, L. K. Bigelow (Marcel Dekker, New York, 1997), Chap. 5, pp. 147–192.
- [70] D. T. Morelli, in *Chemistry and Physics of Carbon*, edited by P. A. Thrower (Marcel Dekker, New York, 1992), Vol. 24, Chap. 2, pp. 45–109.